ORDEM DOS ENGENHEIROS
INFORMAÇÃO GEOESPACIAL PARA AS GERAÇÕES FUTURAS
OPORTUNIDADES E DESAFIOS
VIII CNCG
CONFERÊNCIA NACIONAL DE CARTOGRAFIA E GEODESIA
29 e 30 de outubro de 2015

Deformation monitoring of the Balanegra Fault zone (Betic Cordillera, SE Spain) with Multi-Temporal InSAR

Antonio Miguel RUIZ-ARMENTEROS[1,2,3], J. Manuel DELGADO[3,4], Joaquim J. SOUSA[5], Ramon F. HANSSEN[6], Miguel CARO[7], María Jesús BORQUE[1,2,3], Antonio J. GIL[1,2,3], Jesús GALINDO-ZALDÍVAR[8,9], Carlos SANZ DE GALDEANO[9]

[1] Departamento de Ingeniería Cartográfica, Geodésica y Fotogrametría, Universidad de Jaén
Escuela Politécnica Superior de Jaén, Campus Las Lagunillas s/n, Edif. A3, 23071 Jaén, (Spain)
[2] Centro de Estudios Avanzados en Ciencias de la Tierra CEACTierra, Universidad de Jaén
[3] Grupo de investigación Microgeodesia Jaén, Universidad de Jaén
[4] Progressive Systems Srl, Rome, (Italy)
[5] Escola de Ciências e Tecnologia, Universidade de Trás-os-Montes e Alto Douro
Quinta de Prados Apartado 1013, 5001-801 Vila Real, (Portugal)
[6] Department of Geoscience and Remote Sensing, Delft University of Technology, Stevinweg 1
2628CN, Delft, P.O. Box 5048, 2600GA Delft, (The Netherlands)
[7] Department of Radar Technology, TNO, The Hague, (The Netherlands)
[8] Departamento de Geodinámica, Facultad de Ciencias, Universidad de Granada
Campus de Fuentenueva, s/n, 18071 Granada, (Spain)
[9] Instituto Andaluz de Ciencias de la Tierra, Facultad de Ciencias, CSIC-Universidad de Granada
Campus de Fuentenueva, s/n, 18071 Granada, (Spain)

(amruiz@ujaen.es; JoseManuel.DelgadoBlasco@esa.int; jjsousa@utad.pt; R.F.Hanssen@tudelft.nl; miguel.carocuenca@tno.nl; mjborque@ujaen.es; ajgil@ujaen.es; jgalindo@ugr.es; csanz@ugr.es)

Keywords: Radar interferometry, deformation, InSAR, Balanegra fault

Abstract: The internal zones of the Betic Cordilleras show a present-day relief that is mainly controlled by kilometer-size, E-W to NE-SW trending folds. Field evidence has shown that the growth of the folds is coeval with fault development. One of them is the Balanegra Fault, which is located at the southwest of the Sierra of Gádor, and belongs to a set of NW-SE oriented faults that show a main dip-slip (normal) kinematics with a linked NE-SW extension, developed in response to the current stress field imposed by the African-Eurasian oblique convergent motion (4-5 mm/yr in NW-SE direction). This fault, considered as one of the most active structures in the area, displays tectonic, geomorphological, and seismological evidence of recent motion, with slip rate values in the order of 0.4 mm/yr estimated according to historical seismicity, although recent levelling surveys carried out along this fault between 2006 and 2012 have determined lower rates. It constitutes the possible source of four moderate-size earthquakes (Mw 4.5 – 6.7) over the last five centuries at a minimum ~100 yr recurrence interval. The 5 – 6.5 maximum magnitude earthquake expected for this low slip rate fault in a minimum time span of ~100 yr represents a seismic risk that should be taken into account for future hazard-mitigation decision making. In this study, we apply Multi-Temporal InSAR by means of ERS-1/2 SAR and Envisat ASAR data to study the deformation pattern in this area in the period 1992-2010. The mean LOS velocity time series for the points located on the right of the main trace of the Balanegra Fault show a deformation trend close to 0 mm/yr with both satellite data whereas the time series of the points on the left (closest block to the sea) show a subsidence trend in the order of 1-3 mm/yr in the whole period of analysis.

1. Introduction

The internal zones of the Betic Cordilleras (southern Spain), located along the oblique convergent African–Eurasian plate boundary, are characterized by a tectonic setting where compressional structures developed simultaneously with the extensional ones, in response to the present-day motion between Iberia and Africa (4–5 mm/yr plate convergence in a NW–SE direction, Argus *et al*., 1989; DeMets *et al*., 1990, 1994).

After some geophysical and geological studies in this area, it has been assessed that some of the most active features are related to the subduction of the continental crust of the Iberian Massif below the Betic Cordilleras (Morales *et al*., 1999). The stress field originates moderately active NW–SE to WNW–ESE normal and normal–oblique faults associated with seismicity (Sanz de Galdeano *et al*., 1995; Galindo-Zaldívar *et al*., 1999, 2003; Marín-Lechado *et al*., 2005; Pedrera *et al*., 2011, 2012a) which presumably have a very low slip rate given the regional low strain magnitude and the width of the sector subjected to deformation (more than 300 km) (Fig. 1). While regional horizontal deformations have been determined by GPS measurements (Fadil *et al*., 2006; Vernant *et al*., 2010), high-precision levelling is used to accurately quantify the vertical local deformation caused by normal faults. Although regional levelling profiles are available (Giménez *et al*., 2009), slip along local active structures remains to be demonstrated in this Cordillera.

In particular, in the northern Alborán Sea, the activity of these faults bears relevance for natural hazards (Goy and Zazo, 1986; Gràcia *et al*., 2012), and some of these active normal faults are monitored onshore by non-permanent GPS networks and high-precision levelling profiles (Gil *et al*., 2002; Galindo-Zaldívar *et al*., 2003; Alfaro *et al*., 2006; Marín-Lechado *et al*., 2010; Galindo-Zaldívar *et al*., 2013).

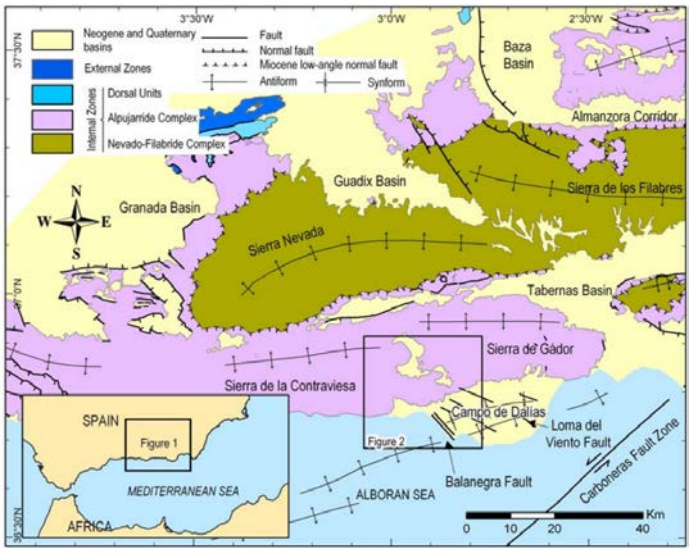

Figura 1 – Geological map of the southeastern Betic Cordilleras (From: Marín-Lechado *et al*., 2010).

The best evidence of an active fault in this area is found to the southwest of Sierra de Gádor, where the roughly NW-SE oriented Balanegra Fault Zone (BFZ) (Fig. 2) controls the position and setting of the coast line and may be associated to the 1993–1994 seismic sequence described by Stich *et al*. (2001). The distribution of earthquakes during this sequence and the following seismicity until 1998 reveals well-defined lineaments striking N120–130º E parallel to the BFZ. This fault zone is interpreted as an extensional feature developed in response to the current stress field imposed by the oblique motion of Africa with respect to Eurasia as mentioned before. Galindo-Zaldívar *et al*. (2013) determined its vertical rate in the main onshore fault segment by repeated measurements between 2006 and 2012 along two high precision levelling profiles (called Greenhouses and Old Guard Fortress, Fig. 3).

The southern Old Guard Fortress profile, near the source of the 1994 (Mw = 4.9) earthquake, undergone a lower deformation than the Greenhouses profile. In any case, the mean rate of deformation determined for the BFZ is lower than the roughly 0.4 mm/yr

highest estimation suggested by historical seismicity. They concluded that part of the historical earthquakes could occur out of the BFZ, or that stress accumulation with low related deformations occurs during interseismic periods. The 5–6.5 maximum magnitude expected for this fault in a minimum time span of ~100 yr represents a seismic risk that should be taken into account for future hazard-mitigation decision making.

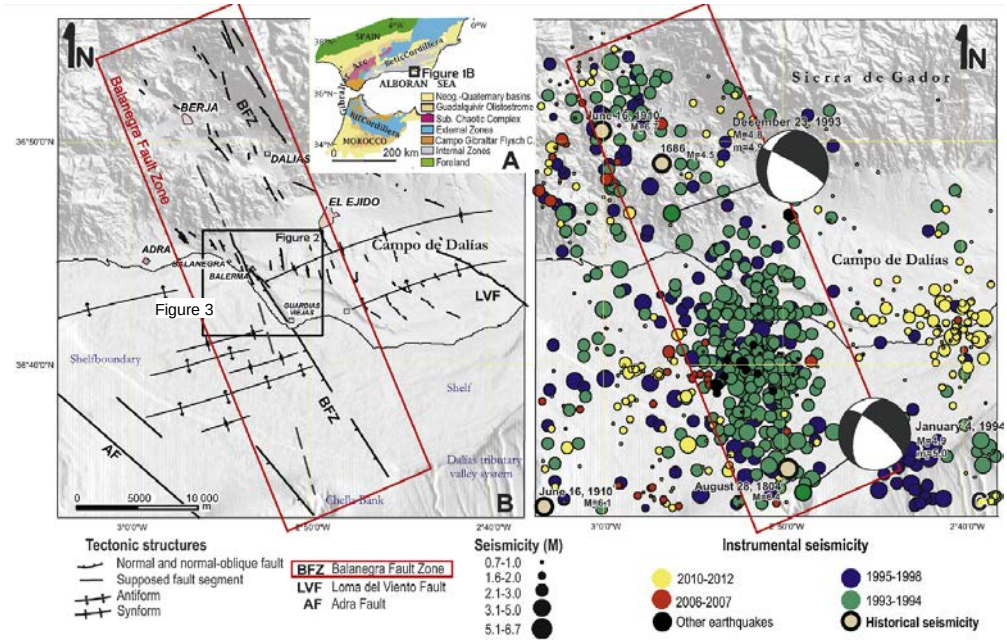

Figura 2 – Geological setting of the study area. (A) Regional geological setting.
(B) Digital elevation model with faults (black lines) recognised on field and lineaments offshore from slope gradient.
(C) Seismicity within and near Balanegra Fault Zone. The aftershocks of the 1993–1994 series, seismicity from 1994 to 1998, the cluster of microseismicity of 2006–2007 and the seismic period of 2010–2012 are differentiated.
(From: Galindo-Zaldívar *et al*., 2013).

Classical surveys, although allow for the detection of very small surface deformations, they are rather time-consuming and thus expensive. The introduction of space-geodetic techniques like GPS and the interferometric use of Synthetic Aperture Radar (InSAR) have offered new opportunities for precise deformation monitoring. In particular, using the InSAR technique at relatively low costs (when compared to leveling) relatively large areas can be monitored providing vertical displacements between coherent points in two SAR acquisitions (images). The introduction of this relatively new technique opened a world of applications in geoscience, and provided an alternative to the traditional optical methods of imaging, which need solar illumination and cloudless skies. Nowadays, InSAR has matured to a widely used geodetic technique for measuring the Earth's surface, including topography and deformation, among other reasons, due to the amount of data available spanning almost two decades. Multi-temporal InSAR techniques (MTI) are gaining popularity as tool for deformation measurements due to its ability to overcome the limitations of the conventional InSAR. MTI techniques profited SAR scenes regular acquisitions since 1991 (ERS-1), which allowed the establishment of large archives of SAR images permitting the implementation of long temporal studies, by the use of long time series stacks.

This paper shows the results of a MTI analysis by means of ERS-1/2 SAR and Envisat ASAR data to study the deformation pattern in the BFZ in the period 1992-2010.

2. Geodynamics setting

The Campo de Dalías is widely deformed by NW–SE and WNW–ESE trending normal and oblique-slip faults that have been active since the Pleistocene. These faults are coeval with the development of ENE–WSW open folds (Figs. 1 and 2) (Marín-Lechado *et al*., 2005, 2007; Martínez-Díaz and Hernández-Enrile, 2004; Pedrera *et al*., 2012b). The BFZ is formed by generally southwestward

dipping fault segments trending NW–SE, which extends from the north of Berja towards the Alborán Sea, controlling the western end of the Sierra de Gádor antiform and the NW–SE oriented straight morphology of the coastline (Fig. 2B).The 1993–1994 seismic series occurred along the BFZ (Fig. 2C). Fault slip rate values estimated in the fault segment that limits the western border of the Sierra of Gádor are comprised between 0.1 and 0.3 mm/yr (Martínez-Díaz and Hernández-Enrile, 2004), in the northern part of BFZ. Southwards, the BFZ gives rise to a 6-km-long N 140º E oriented lineament parallel to the coastline, where the difference in topography associated with fault activity is of about 45 m, and Pliocene sediments have cross-bedding laminations dipping up to 30º towards the downthrown block.

Figura 3 – Faults distribution over Goggle Earth in the area of study. Red lines represent levelling profiles for the period 2006-2012. (Galindo-Zaldívar *et al*., 2013). Black lines connect points from which their MTI-InSAR mean LOS velocities time-series have been retrieved. These points are depicted by triangles.

3. Methodology and dataset

In this work, the Stanford Method for Persistent Scatterers - Multi-Temporal InSAR (StaMPS-MTI) that combines both persistent scatterer (PSI) and small baselines (SB) methods, allowing the identification of scatterers that dominate the scattering from the resolution cell (PS) and slowly-decorrelating filtered phase (SDFP) pixels, was applied.

A DEM with 25 m resolution provided by the Spanish Instituto Geográfico Nacional was used as an external DEM in this study to remove the topographic phase from the differential interferograms. In the same way, the reference phase was computed using highly precise orbit data for ERS-1/2 and Envisat satellites calculated by TU Delft (Scharroo and Visser, 1998) and ESA.

3.1 StaMPS-MTI

The StaMPS framework was initially developed for PS applications in natural terrain (Hooper *et al*., 2004, 2007) and since, has been expanded to include short baseline analysis (Hooper, 2008). StaMPS PSI analysis uses primarily spatial correlation of the phase to identify phase-stable pixels, as opposed to temporal correlation and it does not assume any approximate model of displacements (eg. Ferretti *et al*., 2001; Kampes, 2005). A requirement is that the displacement gradients in space and time should not be steep for proper unwrapping. Once coregistering master and slave images, a series of interferograms is constructed, which also uses the most precise orbit information available. An evaluation of interferometric phase differences in time is done to obtain the potential PS points. Finally, temporally coherent of natural reflectors in SAR images are detected due to their correlated phase behavior over time. Then, the displacement of each individual PS point is estimated by the technique.
In addition, SBAS (Berardino *et al*., 2002) (Small BASeline) analysis aims to detect pixels whose phase decorrelates little over short time intervals. Interferograms having mutual small baselines combinations are created based on the available of image. SBAS method searches to ease phase unwrapping by means of selecting small baselines interferograms and filtering the phases. It creates a network of interferograms to estimate heights and deformation with respect to one single master image.

Finally, StaMPS/MTI combines both sets of results to improve phase unwrapping and the spatial sampling of the signal of interest.

3.2 Data used

The study area is covered by a total of 22 ERS-1/2 SAR scenes from descending satellite track 8, and 32 Envisat ASAR scenes from descending satellite track 416. These SAR images covered the time period between June 1992 and October 2000 (ERS-1/2) and December 2002 to June 2010 (Envisat).

4. Results

We applied the StaMPS-MTI method to the two datasets (ERS-1/2 descending and ASAR descending). For every stack we processed PSI, SB and the combined (PSI+SB) method. In the case of ERS-1/2, we selected the image of 16th November 1999 as master image in the PSI processing. We formed 21 single master interferograms detecting 37574 stable-phase pixels (PS). For the SB processing, the network was composed of 43 interferograms, selecting 16413 SDPF pixels. After their combination and recomputation of the unwrapped phase values, 46308 stable-phase pixels were selected for a regional area of about 22x22 km^2.

In the case of the ASAR dataset, we selected the image of 31th May 2005 as master date. We constructed 31 and 86 interferograms for the PSI and SB processing respectively. In the same way, 85420 and 31294 stable-phase pixels were identified in both processing methods. Finally, for the combined processing, 109613 PS pixels were selected.

The bottom part of the area (Campo de Dalías) is very flat with a medium topography at the north part of the crop (heights from 0 m at sea level to close to 1000 m) and vegetation. No so many phase-stable pixels were detected in the Balanegra Fault Zone due to the presence of many greenhouses. Most of the persistent scatterers in this area are located in urbanized places (Fig. 4). After phase unwrapping step and filtering spatially-correlated noise, a mean velocity line-of-sight LOS rates for each persistent scatterer is calculated relative to a circular reference area (radius of 250 m) located in a stable mountain zone at the northwest of the processed area. In the SB and the combined processing, all the residuals between the unwrapped phase of the interferograms and the estimated ones when redundancy was removed by inverting to a single master network first were found to be in the ±π interval. This absence of spatially-correlated residuals clearly shows the absence of unwrapping errors.

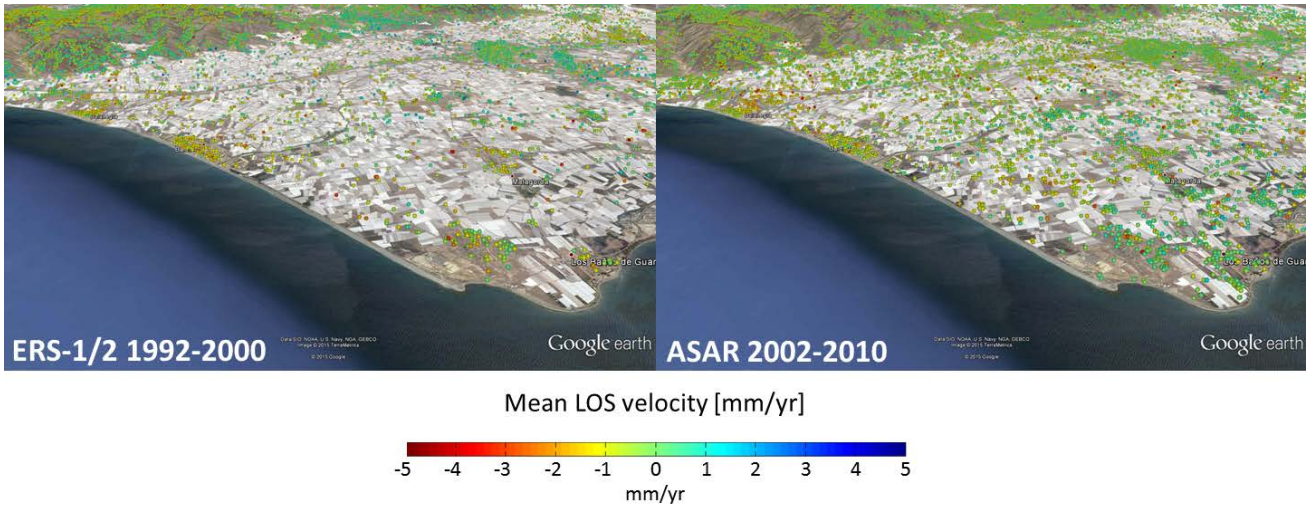

Figura 4 – 3D views of the western part of The Campo de Dalías where many greenhouses are placed in this flat area. At the upper part of the images the beginning of The Sierra de Gádor can be seen. The images represent the mean LOS velocity of deformation.

Fig. 5 shows a detailed view of the mean LOS velocity deformation maps in the BFZ for ERS-1/2 and ASAR results. Very few persistent scatterers were detected in the area where the levelling profiles are measured what makes difficult the comparison of the results of both methodologies. In particular, no PS were detected the Old Guard Fortress profile. In these figures, the time series of the points selected for MTI-InSAR analysis (Fig. 3) are shown on the left and right borders. The location of the points is the same in both ERS-1/2 and Envisat plots. The mean LOS velocity time series for the points located on the right of the main trace of the

Balanegra Fault (A', B', C', D' and 994) show a deformation trend close to 0 mm/yr in both periods (ERS-1/2 and Envisat) whereas the time series of the points on the left (A, B, C, D and 992), the closest block to the sea, show a subsidence trend in the order of 1-3 mm/yr also in the whole period of analysis (1992-2010).

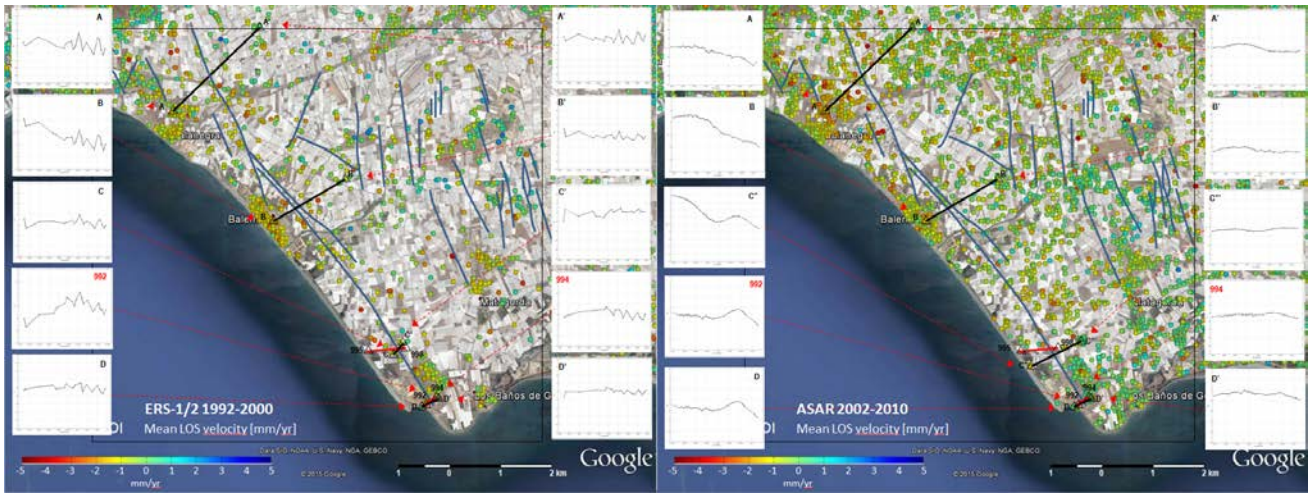

Figura 5 – Mean LOS velocity deformation maps in the BFZ for both the ERS-1/2 and Envisat periods. On the borders, the deformation time series for some point in both sides of the main trace of the Zafarraya Fault.

5. Conclusions

The Sierra de Gádor is an example of associated faults and folds. South of this mountain range, the Campo de Dalias and surrounding areas comprise one of the most interesting zones for a characterization of present deformation as well as the relationship between the different compressive and extensional structures, folds and faults. The best evidence of an active fault in this area is found to the west of the Campo de Dalías, where the roughly NW-SE oriented Balanegra Fault controls the position and setting of the coast line and may be associated to the 1993–1994 seismic sequence described by Stich *et al.* (2001).

Galindo-Zaldívar *et al.* (2013) determined its vertical rate in the main onshore fault segment by repeated measurements between 2006 and 2012 along two high precision levelling profiles. The mean rate of deformation determined for the BFZ with this levelling is lower than the roughly 0.4 mm/yr highest estimation suggested by historical seismicity. On the other hand, radar interferometry, by means of Multi-temporal techniques can detect surface deformations on the order of 1 mm/yr, in the best scenarios, with a wide temporal and spatial coverage, and a no cost, which makes them very competitive against classical geodetic methods. In this work, some Multi-Temporal InSAR techniques have been applied to monitor the deformation of this area. In general, there have not been detected so many persistent scatterers in the BFZ due to the great presence of greenhouses. Nevertheless, the amount of persistent scatterers in this area is enough to detect a subsidence on the order of 1-3 mm/yr of the SW block of the Balanegra fault with respect to the NE block in the period 1992-2010. This subsidence possibly related to the BFZ activity has to be analyzed in deep because the 5–6.5 maximum magnitude expected for this fault in a minimum time span of ~100 yr represents an important seismic risk for the region

Acknowledgements

SAR data are provided by the European Space Agency (ESA) in the scope of 7629 CAT-1 project. This research was supported by PRX14/00340, Consolider–Ingenio 2010 Programme (Topo-Iberia project) CSD2006–0041 (Consolider), AYA2009-10209 and AYA2010-15501 projects from Ministerio de Ciencia e Innovación (Spain), and by the RNM-282, RNM148 and RNM-5388 research groups from the Junta de Andalucía (Spain). DEM data were provided by Spanish IGN.

References

Alfaro, P.; Estevez, A.; Blázquez, E.B.; Borque, M.J.; Garrido, M.S.; Gil, A.J.; Lacy, M.C.; Ruiz, A.M.; Giménez, J.; Molina, S.; Rodríguez-Caderot, G.; Ruiz-Morales, M.; Sanz de Galdeano, C. (2006). Geodetic control of the present tectonic deformation of the Betic Cordillera (Spain). In: Sansò, F., Gil, J. (Eds.), Geodetic Deformation Monitoring: from Geophysical to Engineering Roles, IAG Symposium Jaén, Spain, vol. 131, pp. 209–216.

Argus, D.F.; Gordon, R.G.; DeMets, C.; Stein, S. (1989). Closure of the Africa–Eurasia–North America plate motion circuit and tectonics of the Gloria fault. Journal of Geophysical Research 94, 5585–5602.

Berardino, P.; Fornaro, G.; Lanari, R.; Sansosti, E. (2002). A new algorithm for surface deformation monitoring based on small baseline differential SAR interferograms. IEEE Transactions on Geoscience and Remote Sensing 40(11), 2375 – 83.

DeMets, C.; Gordon, R.G.; Argus, D.F.; Stein, S. (1990). Current plate motions. Geophysical Journal International 101, 425–478.

DeMets, C.; Gordon, R.G.; Argus, D.F.; Stein, S. (1994). Effect of recent revisions to the geomagnetic reversal time scale on estimates of current plate motions. Geophysical Research Letters 21, 2191–2194.

Fadil, A.; Vernant, P.; McClusky, S.; Reilinger, R.; Gomez, F.; Ben Sari, D.; Mourabit, T.; Feigl, K.; Barazangi, M. (2006). Active tectonics of the Western Mediterranean: GPS evidence for roll back of a delaminated subcontinental slab beneath the Rif Mountains, Morocco. Geology 34, 529–532.

Ferretti, A.; Prati, C.; Rocca, F. (2001). Permanent Scatters in SAR Interferometry. IEEE Transactions on Geoscience and Remote Sensing 39(1), 8-20.

Galindo-Zaldívar, J.; Jabaloy, A.; Serrano, I.; Morales, J.; González-Lodeiro, F.; Torcal, F. (1999). Recent and present-day stresses in the Granada Basin (Betic Cordilleras): example of a late Miocene-present-day extensional basin in a convergent plate boundary. Tectonics 18, 686–702.

Galindo-Zaldívar, J.; Gil, A.J.; Borque, M.J.; González-Lodeiro, F.; Jabaloy, A.; Marín-Lechado, C.; Ruano, P.; Sanz de Galdeano, C. (2003). Active faulting in the internal zones of the central Betic Cordilleras (SE, Spain). Journal of Geodynamics 36, 239–250.

Galindo-Zaldívar, J.; Borque, M.J.; Pedrera, A.; Marín-Lechado, C.; Gil, A.J.; López-Garrido, A.C. (2013). Deformation behaviour of the low-rate active Balanegra Fault Zone from high-precision levelling (Betic Cordillera, SE Spain). Journal of Geodynamics 71, 43-51.

Gil, A.J.; Rodríguez-Caderot, G.; Lacy, C.; Ruiz, A.; Sanz, C.; Alfaro, P. (2002). Establishment of a non-permanent GPS network to monitor the deformation in Granada Basin (Betic Cordillera, Southern Spain). Studia Geophysica and Geodetica 46,395–410.

Giménez, J.; Borque, M.J.; Gil, A.J.; Alfaro, P.; Estévez, A.; Suriñach, E. (2009). Comparison of long-term and short-term uplift rates along an active blind reverse fault zone (Bajo Segura, SE Spain). Studia Geophysica and Geodaetica 53, 81–98.

Goy, J.L.; Zazo, C. (1986). Synthesis of the Quaternary in the Almería litoral neotectonic activity and its morphologic features, western Betics, Spain.Tectonophysics 130, 259–270.

Gràcia, E.; Bartolome, R.; Lo Iacono, C.; Moreno, X.; Stich, D.; Martínez-Díaz, J.J.; Bozzano, G.; Martínez-Loriente, S.; Perea, H.; Diez, S.; Masana, E.; Dañobeitia, J.J.; Tello, O.; Sanz, J.L.; Carreño, E., EVENT-SHELF Team (2012). Acoustic and seismic imaging of the Adra Fault (NE Alboran Sea): in search of the source of the 1910 Adra earthquake. Natural Hazards and Earth System Science 12, 3255–3267.

Hooper, A.; Zebker, H.; Segall, P.; Kampes, B. (2004). A new method for measuring deformation on volcanoes and other natural terrains using InSAR persistent scatterers, Geophysical Research Letters, 31(23), doi:10.1029/2004GL021737.

Hooper, A.; Segall, P.; Zebker, H. (2007). Persistent scatterer InSAR for crustal deformation analysis with application to Volcán Alcedo, Galápagos, J. Geophys. Res. Lett., 112 (B07407), doi:10.1029/2006JB004763.

Hooper, A. (2008). A multi-temporal InSAR method incorporating both persistent scatterer and small baseline approaches, Geophysical Research Letters (35), L16, 302, doi:10.1029/2008GL03465.

Kampes, B.M. (2005). Displacement Parameter Estimation using Permanent Scatterer Interferometry, PhD Thesis, Delft University of Technology. The Netherlands.

Marín-Lechado, C.; Galindo-Zaldívar, J.; Rodríguez-Frernández, L.R.; Serrano, I.; Pedrera, A. (2005). Active faults, seismicity and stresses in an internal boundary of a tectonic arc (Campo de Dalías and Níjar, southeastern Betic Cordilleras, Spain). Tectonophysics 396, 81–96.

Marín-Lechado, C.; Galindo-Zaldívar, J.; Rodríguez-Fernández, L.R.; Pedrera, A. (2007). Mountain front development by folding and crustal thickening in the internal zone of the Betic Cordillera–Alboran Sea boundary. Pure and Applied Geophysics 166, 1–21.

Marín-Lechado, C.; Galindo-Zaldívar, J.; Gil, A.J.; Borque, M.J.; de Lacy, C.; Pedrera, A.; López-Garrido, A.C.; Alfaro, P.; García-Tortosa, F.; Ramos, I.; Rodríguez-Caderot, G., Rodríguez-Fernández, J.; Ruiz-Constán, A.; Sanz de Galdeano-Equiza, C. (2010). Levelling profiles and a GPS network to monitor the active folding and faulting deformation in the Campo de Dalías (Betic Cordillera, Southeastern Spain). Sensors 10, 3504–3518.

Martínez-Díaz, J.J.; Hernández-Enrile, J.L. (2004). Neotectonics and morphotectonicsof the southern Almería region (Betic Cordillera-Spain) kinematic implications. International Journal of Earth Sciences 93, 189–206.

Morales, J.; Serrano, I.; Jabaloy, A.; Galindo-Zaldívar, J.; Zhao, D.; Torcal, F.; Vidal, F.; Gonzñalez-Lodeiro, F. (1999). Active continental subduction beneath the Betic Cordillera and the Alborán Sea. Geology 27, 735–738.

Pedrera, A.; Ruiz-Constán, A.; Galindo-Zaldívar, J.; Chalouan, A.; Sanz de Galdeano, C.; Marín-Lechado, C.; Ruano, P.; Benmakhlouf, M.; Akil, M.; López-Garrido, A.C.; Chabli, A.; Ahmamou, M.; González-Castillo, L. (2011). Is there an activesubduction beneath the Gibraltar orogenic arc? Constraints from Pliocene to present-day stress field. Journal of Geodynamics 52, 83–96.

Pedrera, A.; Galindo-Zaldívar, J.; Marín-Lechado, C.; García-Tortosa, F.J.;, Ruano, P., López-Garrido, A.C.; Azañón, J.M.; Peláez, J.A.; Giaconia, F. (2012a). Recent and active faults and folds in the central–eastern internal zones of the Betic Cordillera. Journal of Iberian Geology 38, 191–208.

Pedrera, A.; Marín-Lechado, C.; Stich, D.; Ruiz-Constán, A.; Galindo-Zaldívar, J.; Rey-Moral, C.; Mancilla, F. (2012b). Nucleation, linkage and active propagation of a segmented Quaternary normal-dextral fault: the Loma del Viento fault (Campo de Dalías, Eastern Betic Cordillera, SE Spain). Tectonophysics 522–523, 208–217.

Sanz de Galdeano, C.; López Casado, C.; Delgado, J.; Peinado, M.A. (1995). Shallow seismicity and active faults in the Betic Cordillera. A preliminary approach to seismic sources associated with specific faults. Tectonophysics 248, 293–302.

Scharroo, R.; Visser, P. (1998). Precise orbit determination and gravity field improvement for the ERS satellites. Journal of Geophysical Research 103 (C4), 8113–8127.

Stich, A.G.; Alguacil, G.; Morales, J. (2001). The relative locations of multiplets inthe vicinity of the Western Almería (southern Spain) earthquake series of 1993–1994. Geophysical Journal International 146, 801–812.

Vernant, P.; Fadil, A.; Mourabit, T.; Ouazard, D.; Koulalid, A.; Martin-Dávila, J.; Garate, J.; McClusky, S.; Reilinger, R. (2010). Geodetic constraints on active tectonics of the western Mediterranean: implications for the kinematics and dynam-ics of the Nubia–Eurasia plate boundary zone. Journal of Geodynamics 49,123–129.